Author Manuscript

Author Manuscript

Author Manuscript

Author Manuscript

HHS Public Access

Author manuscript

*J Med Virol*. Author manuscript; available in PMC 2024 July 01.

Published in final edited form as:

*J Med Virol*. 2023 July ; 95(7): e28957. doi:10.1002/jmv.28957.

# NAC1 confines virus-specific memory formation of CD4+ T cells through the ROCK1-mediated pathway

**Liqing Wang**[1,2], **Hao-Yun Peng**[1,2], **Jugal Kishore Das**[1], **Anil Kumar**[1], **Yijie Ren**[1], **Darby J Ballard**[1], **Xiaofang Xiong**[1], **Wen Yang**[3], **Xingcong Ren**[4], **Paul de Figueiredo**[1,5], **Jin-Ming Yang**[4,#], **Jianxun Song**[1,#]

[1]Department of Microbial Pathogenesis and Immunology, Texas A&M University Health Science Center, Bryan, TX 77807, USA

[2]Department of Biochemistry and Biophysics, Texas A&M University, College Station, TX 77843, USA

[3]Imgen BioSciences, Fall River, MA 02723, USA

[4]Department of Toxicology and Cancer Biology, Department of Pharmacology and Nutritional Science, and Markey Cancer Center, University of Kentucky College of Medicine, Lexington, KY 40536, USA

[5]Department of Veterinary Pathobiology, Texas A&M University, College Station, TX 77845, USA

## Abstract

Nucleus accumbens-associated protein 1 (NAC1), a transcriptional co-factor, has been found to play important roles in regulating regulatory T cells, $CD8^+$ T cells, and antitumor immunity, but little is known about its effects on T cell memory. In this study, we found that NAC1 expression restricts memory formation of $CD4^+$ T cells during viral infection. Analysis of $CD4^+$ T cells from wild-type (WT) and NAC1-deficient ($^{-/-}$) mice showed that NAC1 is essential for T cell metabolism, including glycolysis and oxidative phosphorylation, and supports $CD4^+$ T cell survival *in vitro*. We further demonstrated that a deficiency of NAC1 downregulates glycolysis and correlates with the AMPK-mTOR pathway and causes autophagy defective in $CD4^+$ T cells. Loss of NAC1 reduced the expression of ROCK1 and the phosphorylation and stabilization of BECLIN1. However, a forced expression of ROCK1 in $NAC1^{-/-}$ $CD4^+$ T cells restored autophagy and the activity of the AMPK-mTOR pathway. In animal experiments, adoptively transferred $NAC1^{-/-}$ $CD4^+$ T cells or $NAC1^{-/-}$ mice challenged with VACV showed enhanced formation of VACV-specific $CD4^+$ memory T cells compared to adoptively transferred WT $CD4^+$ T cells

[#]**Correspondence to:** Jianxun Song or Jin-Ming Yang, MREB II, Room 3344, 8447 Riverside Pkwy, Bryan, TX 77807. Tel: +1 979 436 0633; Fax: +1 979 436 0991; jus35@tamu.edu, 1095 V.A. Drive, 306 Health Science Research Building, Lexington, KY 40536-0305. Tel: +1 859 562 2154; Fax: +1 859 257 6030; jyang@uky.edu.

**Author Contributions:** J.S. and J-M. Y. designed the experiments, analyzed data, and contributed to the writing of the paper. P.D.F. and W. Y. contributed to the writing of the paper. L.W., H-Y. P, A.K., J.K.D., and Y.R. and performed the experiments. D.J.B., X.X. and X.R. analyzed data.

The authors have declared that no conflict of interest exists.

**Institutional Review Board Statement:** The study was conducted according to the guidelines of the Declaration of Helsinki, and approved by the Institutional Review Board of The Texas A&M University Animal Care Committee (IACUC; #2018–0006; 03/13/2018).

**Informed Consent Statement:** Not applicable.

Author Manuscript Author Manuscript Author Manuscript Author Manuscript

or WT mice. This memory T cell formation enhancement was abrogated by forcing expression of ROCK1. Our study reveals a novel role for NAC1 as a suppressor of $CD4^+$ T cell memory formation and suggests that targeting NAC1 could be a new approach to promoting memory $CD4^+$ T cell development, which is critical for an effective immune response against pathogens.

### Keywords

NAC1; $CD4^+$ T cells; memory formation; cellular metabolism; ROCK1

## Introduction

Hosts infected by pathogens such as viruses and bacteria trigger adaptive immune responses that play a crucial role during the defensive process [1]. After the pathogens have been eliminated, the host generates memory for the invading pathogens in preparation for future possible reinfection. Upon encountering reinfection of the pathogens, the memory T cells will be activated quickly and form effective protection [2]. The formation of memory T cells is controlled by a variety of factors such as virus species [3–5], co-stimulation factors [6,7], and transcriptional factors [8]. For instance, the chickenpox and smallpox vaccine can provide full protection for more than 5 years [4,5]. Nevertheless, some other viral vaccines only maintain short-term protection. It is known that many transcriptional factors, such as T Cell factor 1 (TCF1) and interferon regulatory factor 4 (IRF4), can affect T cell memory formation [8,9], and targeting these transcription factors may improve T cell memory and prolong the efficacy of vaccines.

Nucleus accumbens-associated protein 1 (NAC1) is a transcriptional factor belonging to the BTB/POZ (**b**road complex, **t**ramtrack, **b**ric-a-brac/**po**xvirus and **z**inc finger; hereafter abbreviated BTB) gene family. NAC1 is a nuclear protein harboring an *N*-terminal BTB/POZ and a *C*-terminal BEN (BANP, E5R, and NAC1) domain [10]. The highly conserved BTB/POZ domain enables NAC1 dimerization, and the formation of the homodimer complex participates in various biological processes, including transcription regulation [11], protein degradation *via* ubiquitination, cell proliferation, and apoptosis. For example, NAC1 regulates the pluripotency of stem cells such as embryonic stem cells (ESCs) and pluripotent stem cells (PSCs) [12,13], and promotes mesendodermal and represses neuroectodermal fate selection in ESCs, through cooperation with other pluripotency transcription factors, Oct4, Sox2, and Tcf3 [14]. We have recently reported the roles of NAC1 in suppressing regulatory T cell (Treg)-mediated immune tolerance [15] and in restraining $CD8^+$ T cell memory formation during vaccinia virus (VACV) infection [16]. In the current study, we found that expression of NAC1 confines the memory formation of $CD4^+$ T cells as well as modulates their metabolism, survival, and autophagy. Importantly, these roles of NAC1 are mediated via ROCK1-mediated regulation of BECLIN1 and the activity of AMPK-mTOR. Thus, NAC1 may represent a novel repressor of memory $CD4^+$ T cell formation.

Author Manuscript Author Manuscript Author Manuscript Author Manuscript

## Material and methods

### Cell lines and cell culture

HeLa cells or Vero C1008 were cultured in Minimum Essential Media (MEM) medium (Sigma) with 10% FBS, 1% penicillin-streptomycin, and 0.03% L-glutamine. The Platinum-E cell line was grown in Dulbecco's Modified Eagle Medium (Sigma) with 10% FBS, 1% Penicillin-streptomycin, and 2 mM L-glutamine. Naive $CD4^+$ T cells were isolated from the mice's spleen and lymph node by Mojosort Naive $CD4^+$ T Cell Isolation Kit (BioLegend #480040). Then the T cells were stimulated with coated anti-CD3 (BioLegend #100340) and soluble 4 μg/mL anti-CD28 (BioLegend #102116) in RPMI medium (Invitrogen) with 1% NEAA, 10% FBS, 1% Penicillin-streptomycin, 55 mM 2-ME, and 2 mM L-glutamine.

### Animal maintenance

Wild-type C57BL/6 (B6 $Thy1.2^+$), and congenic mice (B6 $Thy1.1^+$) were purchased from Jackson Lab (Bar Harbor, ME). $NAC1^{-/-}$ mice were generated by Jian-long Wang and crossed with C57BL/6 (B6 $Thy1.2^+$) mice. All mice strains were maintained at Texas A&M University Laboratory Animal Resources and Research Facility. All the animal work was conducted under the regulations of the Texas A&M University Animal Care Committee and the Association for the Assessment and Accreditation of Laboratory Animal Care (IACUC #2018–0065).

### Chemicals

Dactolisib (PI3K inhibitor #S1009), MK-2206 2HCl (AKT inhibitor #S1078), OSU-03012(PDK1 inhibitor #S1106) were purchased from Selleckchem. Bafilomycin A1 (CST #54645) was purchased from Cell Signaling.

### Cell staining and flow cytometry

For flow analysis of the T cells from mice, the spleens and lymph nodes were collected, smashed, and filtered with 40 μm cell strainers. The cell staining protocols were based on BioLegend standard staining protocol. Cells were stained in cell staining buffer (BioLegend #420201) for 15 minutes on ice with flow antibodies (Abs). The vaccinia virus tetramer (H3L PGVMYAFTTPLISFF) staining was accomplished at room temperature for 30 minutes. All the flow analyses were conducted in SMACC of TAMU using BD Fortessa X-20 flow cytometer and analyzed by FlowJo software. The detailed flow Abs list was attached in Supplementary Table 1.

### Measurement of cell survival and cytokine secretion

The cell recovery and viability were counted with Bio-Rad cell counter under trypan blue staining. For the analysis of the intracellular cytokines, the isolated T cells were cultured for 2 days and treated with Brefeldin A (BioLegend #420601) for 12 hours before analysis. First the cells were stained with surface markers, then the cells were fixed with fixation buffer (BioLegend #420801) and permeabilized with a permeabilization buffer (BioLegend #421002). After the intracellular staining with IL-2 and IFN-γ flow Abs, T cells were analyzed by flow cytometry.

Author Manuscript Author Manuscript Author Manuscript Author Manuscript

### Seahorse metabolic analysis

Both cell glycolytic rate (#103346–100) and mitochondrial stress (#103010–100) were tested by Agilent Seahorse Kits. The experiments were conducted according to the Agilent Seahorse Kits User Guide. $CD4^+$ T cells were stimulated and cultured for 3 days. Then $2X10^5$ cells were seeded into Seahorse XF96 culture plate for each well with Seahorse assay medium, composed of DMEM with 1 mM pyruvate, 2 mM glutamine, and 10 mM glucose. The different drugs are loaded into Seahorse cartridges according to their injection sequence. For each independent experiment, drugs were injected at different time points.

### Western blotting and immunoprecipitation

The cells were lysed in M-PER™ Mammalian Protein Extraction Reagent (Thermo Fisher #78501) and proteins supernatant was collected after centrifugation. The protein concentration was then measured with the BCA protein assay (Thermo Fisher #23225). Then the proteins were separated with 4%−12% SDS-PAGE gels and transferred to 0.22 μm PVDF membranes. The membrane was blocked in 5% dry milk and incubated with primary Abs in 5% BSA overnight at 4°C. The secondary HRP conjugated Abs were incubated at room temperature for 1 hour. Then the membrane was detected with Pierce ECL Detecting Kit (Thermo Fisher #32106) with LI-COR imaging system. For BECLIN1 immunoprecipitation, the extracted protein was first formed in a complex with the Ab at 4°C overnight. Then the beads were incubated with protein-antibody complex for 4 hours at 4°C. The protein was then eluted from the beads by the sample buffer under 95°C before being loaded into the SDS-PAGE gel. The detailed Abs usage list is attached in Supplementary Table 2.

### Confocal imaging

The WT or $NAC1^{-/-}$ $CD4^+$ T cells were stimulated and cultured for three days; then the $CD4^+$ surface marker was stained. The T cells were fixed, permeabilized, stained with the P62 Ab, and mounted with DAPI staining. The imaging was performed using Olympus Fluoview FV3000 Confocal Laser Scanning Microscope at TAMU IMIL imaging core facility.

### Transmission Electronic Microscopy (TEM) imaging

The WT and $NAC1^{-/-}$ $CD4^+$ T cells on day 3 were used for TEM sample preparation. The cells were fixed, dehydrated, and infiltrated into resin according to the cited protocol with minor modifications [17]. Then the resin pyramids were sectioned and stained before imaging. The JEOL1200 Ex TEM was used for imaging in the TAMU MIC imaging core facility.

### qPCR and RNA microarray

The cell RNA was prepared with RNeasy Mini Kit (Qiagen #74104). TURBO DNA-free Kit (Ambion #AM1907) was used to remove any possible DNA. Then cDNA synthesis was conducted with the High-capacity cDNA Reverse Transcription Kit (Thermo Fisher #4368813). The primers for *Beclin1*: Forward- TTTTCTGGACTGTGTGCAGC Reverse- GCTTTTGTCCACTGCTCCTC [18]. *Pik3c3*: Forward- CTATGGAGAATTTAGTGGAGAG Reverse- CTTCATATGTGAGTTGCTTGG

Author Manuscript Author Manuscript Author Manuscript Author Manuscript

[19]. *Rock1*: Forward- AGAAAGAGGACTTGATTTCCCCGTGC Reverse- ACGGACAAAGCCAGATGGTGGG [20]. *Gapdh*: Forward- GTTGTCTCCTGCGACTTCA Reverse- GGTGGTCCAGGGTTTCTTA.

The RT² Profiler™ PCR Array Mouse Autophagy RNA Microarray Kit was purchased from Qiagen (Gene Globe ID - PAMM-084Z).

### Vaccinia virus preparation

The Vaccinia virus Western Reserve strain (VACV-WR) was grown in HeLa cells. After the virus has been collected, the stock was titrated with plaque assay with Vero C1008 cells. The detailed protocol was adapted from a published protocol with some modifications [21]. The virus stock was then stored at −80°C for long-term usage.

### Vector cloning and assembling

The p-ENTR-ROCK1 vector was purchased from Genomics-online (ABIN3433710). The ROCK1 gene was cloned from the p-ENTR-ROCK1 with Gibson ends. The ROCK1 fragment was then assembled with an empty p-MIG vector by NEBuilder® HiFi DNA Assembly Cloning Kit (# E5520S). The p-MIG-ROCK1 vector was amplified and purified with Qiagen HiSpeed Plasmid Maxi Kit (12662).

### Retrovirus transduction

The naive $CD4^+$ T cells were isolated from donor WT C57BL/6 (B6 $Thy1.2^+$) mice and $NAC1^{-/-}$ (B6 $Thy1.2^+$) mice. The p-MIG empty vector or p-MIG-ROCK1 vector was packed with Lipofectamine 3000 (Invitrogen L3000008) and used to treat the platinum-E cell lines at its 80% confluence. The T cells were then activated and cultured for 2 days before transduction. The virus supernatant was collected and filtered with 0.45 μm filter. The half virus supernatant and half T cell medium were used during transduction with 8 μg/mL polybrene and centrifuged for 1.5 hours at X2000g 32°C according to the protocol with minor modification [22]. Transduction was then repeated on day 3. The GFP-positive cells were sorted and used for experiments.

### Adoptive transfer

The recipient $Thy1.1^+$ mice were treated with X-ray irradiation at 4 grays before ACT. Then, T cells were intravenously injected into the recipient mice. At the same time, the mice were intraperitoneally injected with VAVC ($2X10^6$ PFU/mouse). After 35 days, the mixed spleen and lymph nodes were collected from each mouse. The total cell number was counted by Bio-Rad cell counter. The cells were then stained with Thy1.2, CD44, CD69, and CD197 at 4°C. After that, the cells were stained with vaccinia virus class II tetramer at room temperature for 30 minutes.

### CFSE staining

T cells were isolated from pooled LNs and spleen, and labeled with CFSE for 10 min at room temperature. Cells were then activated with precoated anti-CD3 and soluble anti-CD28 Abs. After two days, the samples were analyzed by flow cytometry.

Author Manuscript Author Manuscript Author Manuscript Author Manuscript

### Statistical analysis

Multiple unpaired student T-tests were used to analyze the difference between different groups. A P-value lower than 0.05 was considered significant. GraphPad Prism was utilized to generate the figures.

### Illustration and schematic figures

Figures were designed and generated using Adobe Illustrator; figure illustrations were produced using Biorender Online software.

## Results

### Loss of NAC1 alters the survival, function and metabolism of CD4+ T cells

We observed that NAC1$^{-/-}$ mice maintained a significantly higher percentage of CD4$^{+}$ T cells and a lower percentage of CD8$^{+}$ T cells (Figure 1A–1B). Upon activation with plate-coated anti-CD3 Ab and soluble anti-CD28 Ab, naive CD4$^{+}$ T cells from WT and NAC1$^{-/-}$ mice proliferated and grew. The amount of NAC1$^{-/-}$ CD4$^{+}$ T cells almost doubled after 4 days, but then began to decline; however, the proliferation of CD4$^{+}$ T cells from WT mice peaked on days 5–6, with a 7-fold increase in the cell number (Figure 1C). Additionally, NAC1-mediated T cell survival did not appear to be associated with the anti-apoptotic pathway or programmed cell death, as there were no significant differences in BCL-2 expression (Figure S1A) and in cleaved Caspase-3 and Caspase-3 expression after activation (Figure S1B). Moreover, the secretion of the functional cytokines, IL-2 and IFN-γ from NAC1$^{-/-}$ CD4$^{+}$ T cells was much lower than those from WT CD4$^{+}$ T cells (Figure 1D). Agilent Seahorse Analyses of glycolysis and mitochondrial stress showed that 3 days after activation, the NAC1$^{-/-}$ CD4$^{+}$ T cells had a significantly decreased extracellular acidification rate (ECAR) compared to WT CD4$^{+}$ T cells following ROT/AA injection (Figure 1E–1F). These findings indicated that loss of NAC1 in CD4$^{+}$ T cells led to a reduction in glycolytic activity. The oxidative phosphorylation of the NAC1$^{-/-}$ CD4$^{+}$ T cells was also significantly lower than that of WT CD4$^{+}$ T cells, as evidenced by their reduced oxygen consumption rate (OCR) following carbonyl cyanide p-(tri-fluromethoxy) phenyl-hydrazone (FCCP) injection (Figure 1G–1H). These results demonstrate that deficiency of NAC1 causes alterations in the survival, function, and metabolism of CD4$^{+}$ T cells *in vitro*.

### NAC1 regulates glycolysis of CD4+ T cells and correlates with the AMPK-mTOR pathway

The mTOR pathway is critical in regulating T cell fate and metabolism [23], and autophagy [24]. To investigate whether NAC1-mediated modulation of glycolysis in CD4$^{+}$ T cells is correlated with this pathway, we first compared the mTOR activity of NAC1$^{-/-}$ CD4$^{+}$ T cells with that of WT CD4$^{+}$ T cells by analyzing the p-mTOR/ mTOR ratio ($p<0.05$) (Figure 2A) and the mean fluorescence intensity (MFI) of p-S6, a downstream effector of mTOR (Figure 2B). These experiments showed that CD4$^{+}$ T cells with loss of NAC1 had a significantly lower mTOR activity than WT CD4$^{+}$ T cells (Figure 2A–2B). To determine the roles of the upstream effectors of mTOR, we tested the effects of inhibitors of PI3K, AKT, and PDK1. Figure 2B shows that the differences in the mTOR activity between WT CD4$^{+}$ T cells and NAC1$^{-/-}$ CD4$^{+}$ T cells were compressed by treatment of the cells with

Author Manuscript Author Manuscript Author Manuscript Author Manuscript

the inhibitors of PI3K, AKT or PDK1, suggesting the involvement of the PI3K-AKT/PDK1-mTOR pathways in NAC1-mediated modulation of glycolysis. Nevertheless, there were only small differences in the PI3K and p-AKT/ AKT protein levels between WT and NAC1$^{-/-}$ CD4$^{+}$ T cells (Figure 2C). Similarly, there was no difference in PDK1 expression between WT and NAC1$^{-/-}$ CD4$^{+}$ T cells (Figure 2D). Thus, the PI3K-AKT/PDK1 pathway might not be a controller of mTOR activity, but the AMPK-mTOR pathway appears to contribute to the regulation of mTOR. Notably, NAC1$^{-/-}$ CD4$^{+}$ T cells showed an approximately 5-fold higher p-AMPK/AMPK ratio at day 3 as compared to WT controls (Figure 2E–2F), suggesting that the reduced mTOR activity and glycolysis observed in NAC1$^{-/-}$ CD4 T cells may be a consequence of upregulated AMPK activity.

## NAC1 regulates autophagy in CD4$^{+}$ T cells via the ROCK1-mediated phosphorylation of BECLIN1

As cellular autophagy has a pro-survival role in tumor, and we have previously shown that expression of NAC1 promotes autophagy in tumor cells subjected to stress [25], we inquired whether NAC1 interrupts CD4$^{+}$ T cell autophagy status. Autophagic activity of the naive CD4$^{+}$ T cells activated and cultured for 3 or 6 days was monitored by immunoblot analysis of the autophagic adaptor proteins p-62 and LC3. Figure 3A shows that autophagic activity was lower in the NAC1$^{-/-}$ CD4$^{+}$ T cells than in WT CD4$^{+}$ T cells, as evidenced by a high level of p-62 and lower LC3-II/LC3-I ratio in the absence or presence of bafilomycin. A higher level of p-62 in NAC1$^{-/-}$ CD4$^{+}$ T cells was confirmed by confocal microscopic observation and flow cytometric analysis (Figure 3B–3D). The average p-62 puncta area per 3 cells (Figure 3C) or the total area per approximately 15 cells (Figure S2A) and the MFI for p-62 (Figure 3D) were significantly higher in NAC1-deficient CD4$^{+}$ T cells than their WT counterparts. Decreased autophagic activity in NAC1$^{-/-}$ CD4$^{+}$ T cells was further demonstrated by transmission electron microscope (TEM) observation of autophagosome formation (Figure 3E and Figure S2B), which showed that both the number of autophagosomes and area of autophagosomes were significantly lower in NAC1-deficient CD4$^{+}$ T cells than in controls (* $p<0.05$, ** $p<0.01$) (Figure 3F–3G). These results indicate that loss of NAC1 in CD4$^{+}$ T cells blunts autophagy activity.

To determine how NAC1 modulates autophagy in CD4$^{+}$ T cells, we first examined the expression of BECLIN1, an autophagy initiation protein, in CD4$^{+}$ T cells on days 0, 3 and 6 post-activations. Figure 4A shows that the expression of BECLIN1 was significantly downregulated in NAC1$^{-/-}$ CD4$^{+}$ T cells on days 0 and 6 (* $p<0.05$ and ** $p<0.01$, respectively). On day 3, there seemed to be no significant difference (ns $p>0.05$). PIK3C3, an essential component of the autophagy initiation complex (PIK3C3/BECLIN1 complex), was also downregulated and less stable in NAC1$^{-/-}$ CD4$^{+}$ T cells (Figure 4A and Figure S3B). Further, analysis of autophagy-related genes using RNA microarrays revealed several upregulated autophagy-related genes in NAC1$^{-/-}$ T cells (Figure 4B and Figure S3C). The elevation of *Beclin1* mRNA in NAC1$^{-/-}$ T cells on days 0 or 3 after activation was insignificant compared to controls (Figure 4C), suggesting that the effect of NAC1 on BECLIN1 expression does not occur at the transcriptional level. Interestingly, we found that the phosphorylation of BECLIN1 was significantly decreased in NAC1$^{-/-}$ CD4 T cells (Figure 4D). Furthermore, immunoblot analysis showed that ROCK1, a protein serine/

Author Manuscript Author Manuscript Author Manuscript Author Manuscript

threonine kinase known to phosphorylate BECLIN1 [26], was significantly downregulated in NAC1$^{-/-}$ CD4$^{+}$ T cells (Figure 4E). qPCR showed that mRNA of *Rock1* was also downregulated approximately 3-fold in NAC1$^{-/-}$ CD4 T cells as compared to WT cells (Figure 4F). These results suggest that decreased autophagy observed in NAC1$^{-/-}$ CD4 T cells may result from reduced ROCK1 expression and phosphorylation of BECLIN1.

## NAC1$^{-/-}$ mice show higher survival of VACV-specific CD4$^{+}$ T cells and enhanced formation of VACV-specific memory CD4$^{+}$ T cells

We utilized the vaccinia virus (VACA) to infect the mice and monitor the VACV-specific T cell changes and VACV-specific memory T cell survival. After VACV challenge, WT and NAC1$^{-/-}$ mice responded to viral infection (Figure 5A). The VACV-specific CD4$^{+}$ T cell frequency increased and reached its peak around days 14–21 (Figure 5A and Figure 5C), with the VACV-specific CD4$^{+}$ T cell number reaching a peak around day 21 (Figure 5B). Although NAC1$^{-/-}$ mice generated fewer VACV-specific CD4$^{+}$ T cells than WT mice, the higher frequency of these cells lasted longer than WT mice (Figure 5B–5C). Analysis of the VACV-specific memory CD4$^{+}$ T cells after 35 days found that there was no statistically significant difference in the number of VACV-specific memory CD4$^{+}$ T cells between WT and NAC1$^{-/-}$ mice (Figure 5E); however, NAC1$^{-/-}$ mice maintained a significantly higher frequency of the VACV-specific memory CD4$^{+}$ T cells than WT mice (* $p<0.05$) (Figure 5D–5F). Importantly, most of these VACV-specific memory CD4$^{+}$ T cells were effector memory T cells (CD44$^{high}$CD69$^{low}$CD197$^{low}$) (Figure 5D), with very few cells being the central memory T cells (CD44$^{high}$CD69$^{low}$CD197$^{high}$). NAC1$^{-/-}$ mice also showed a significant increase in resident memory T cells (CD44$^{high}$CD69$^{high}$CD197$^{low}$) (** $p<0.01$) (Figure 5D and Figure 5G). On day 7, VACV-specific CD4$^{+}$ T cells expressed a higher frequency of memory precursor (CD127$^{+}$) cells in NAC1$^{-/-}$ condition (Figure S6A–S6D). These observations suggest an important role for NAC1 as a repressor of CD4$^{+}$ T cell memory formation.

## Adoptive transferred NAC1$^{-/-}$ CD4$^{+}$ T cells generate a higher number and frequency of memory T cells

To test if NAC1$^{-/-}$ CD4$^{+}$ T cell will form better memory and remove the unfavorable conditions for memory formation in NAC1$^{-/-}$ mice, we carried out a study using adoptive transfer of either WT (Thy1.2$^{+}$) or NAC1$^{-/-}$ (Thy1.2$^{+}$) CD4$^{+}$ T cells into Thy1.1$^{+}$ mice (Figure 6A). WT or NAC1$^{-/-}$ CD4$^{+}$ T cells (0.5 million per mouse) were injected into Thy1.1$^{+}$ mice following a 2X10$^{6}$ PFU vaccinia virus (VACV) challenge. Thirty-five days later, the adoptively transferred T cells (Thy1.2$^{+}$) were analyzed by flow cytometry (Figure 6B). The NAC1$^{-/-}$ CD4$^{+}$ T cell group had approximately double the numbers of VACV-specific memory T cells that survived after 35 days (* $p<0.05$) (Figure 6C). The NAC1$^{-/-}$ CD4$^{+}$ T cell transfer group showed a significantly higher frequency of VACV-specific memory T cell population (* $p<0.05$) (Figure 6B & 6D). This same trend was observed in both NAC1$^{-/-}$ mice (Figure 5F) and the NAC1$^{-/-}$ CD4$^{+}$ T cell transfer experiments (Figure 6D), confirming the role of NAC1 in repressing CD4$^{+}$ T cell memory formation. Further, we observed that most of the surviving VACV-specific memory T cells were resident memory T cells (CD44$^{high}$CD69$^{high}$CD197$^{low}$) (Figure 6B), indicating that these VACV-specific memory T cells are more likely to survive in the tissue-resident memory

Author Manuscript Author Manuscript Author Manuscript Author Manuscript

status. However, there was no significant difference between WT and NAC1$^{-/-}$ cell transfer groups in the resident memory T cells (Figure 6E). At the same time, we examined that those VACV-specific memory T cells were not exhausted and expressed similar levels of PD-1 and Tim-3（Figure 6F–6G）. Those VACV-specific T cells were still functional and secret similar levels of IL-2 and IFN-γ compared with WT group (Figure 6H–6I). These *in vivo* experiments clearly demonstrate a role for NAC1 in suppressing the CD4$^+$ T cell memory formation.

### Overexpression of ROCK1 abrogates the enhanced memory T cell formation in NAC1$^{-/-}$ CD4$^+$ T cells

To demonstrate the role of ROCK1 in the NAC1-mediated modulation of T cell memory, we overexpressed ROCK1 in CD4$^+$ T cells using a ROCK1 expression vector. Figure 7A shows that the NAC1$^{-/-}$ CD4$^+$ T cells with forced expression of ROCK1 restored expression of the autophagy protein BECLIN1. Also, we found that forced expression of ROCK1 enhanced BECLIN1 stabilization and rescued BECLIN1 expression in NAC1$^{-/-}$ CD4$^+$ T cells (Figure S5A–S5B). Furthermore, forced expression of ROCK1 in NAC1$^{-/-}$ CD4$^+$ T cells lowered the level of p-AMPK to a similar level as WT cells (Figure 7B & 7C). Moreover, the Thy1.1$^+$ mice receiving adoptive transfer of the p-MIG empty vector-transduced T cells showed that NAC1$^{-/-}$ CD4$^+$ T cells formed higher VACV-specific memory T cell numbers and frequencies than controls (Figure S4A–S4C); however, forced expression of ROCK1 in NAC1$^{-/-}$ CD4$^+$ T cells brought higher memory T cell formation back to similar levels of VACV-specific memory T cell numbers and frequencies (Figure 7D-7F). Also, the reductions of IFN-γ and IL-2 secretion from NAC1$^{-/-}$ CD4$^+$ T cells were partially rescued by forced expression of ROCK1 (Figure S5C–S5F). These experiments demonstrated that ROCK1 has a key role in the NAC1-mediated restriction of the formation of memory CD4$^+$ T cells.

## Discussion

In this study, we demonstrate that absence of NAC1 results in downregulation of CD4$^+$ T cell metabolism including both glycolysis (Figures 1E–1F) and oxidative phosphorylation (Figures 1G–1H). CD4$^+$ T cells require distinct metabolism profiles and autophagy activity during expansion, survival, and memory formation stages [27,28]. Our study shows that NAC1-mediated alteration of glycolysis in CD4$^+$ T cells determines their survival (Figures 1C–1E) and NAC1 supports CD4$^+$ T cell autophagy (Figure 3).

The mTOR pathway has been reported to have important roles in T cell metabolism and fate [23]. We show here that NAC1 interferes with CD4$^+$ T cell glycolysis mainly through the AMPK-mTOR pathway (Figure 2A, Figure 2E–2F) rather than the PI3K-AKT-mTOR pathway (Figure 2C). Previously, anti-apoptotic pathways [29] and apoptotic pathways [30] have been reported to determine T cell survival. However, in our study, it seems that NAC1-mediated regulation of T cell survival is not dependent on these two pathways (Figures S1A–S1B).

Our study demonstrates that NAC1 regulates ROCK1, a protein kinase that has multifaceted functions in different cellular processes. For instance, ROCK1 regulates hepatic lipogenesis

Author Manuscript Author Manuscript Author Manuscript Author Manuscript

by suppressing AMPK activity in the liver [31]. Acting as a kinase, ROCK1 directly controls BECLIN1 phosphorylation and autophagy [26,32]. In this study, we identified that loss of NAC1 interrupts ROCK1 expression, resulting in the disruption of AMPK activity (Figure 2E–2F), BECLIN1 stabilization (Figure 4A) and autophagy (Figure 3). We further show that overexpression of ROCK1 in NAC1$^{-/-}$ CD4$^{+}$ T cells rescues BECLIN1 stabilization and autophagy (Figure 7A, Figure S5A–S5B), and brings highly upregulated p-AMPK to the same level as WT CD4$^{+}$ T cells (Figure 7B-7C). These results support that NAC1 regulates ROCK1 to control CD4$^{+}$ T cells.

The connection between mTOR activity and autophagy in T cells has been reported previously. However, this connection varies in different models and cell types. For example, it was shown that autophagy downregulates mTOR activity in the regulatory T cells [24]. Autophagy defects are discovered in TAX1BP1-deficient effector T cells, leading to mTOR aberration [33]. mTOR is also reported to regulate autophagy by phosphorylating ULK1/ATG13/FIP200 complex [34]. Therefore, based on the previous studies, which proteins are upstream and controlling the others remains undefined. Our results suggest that NAC1$^{-/-}$ CD4$^{+}$ T cells may have both defective mTOR activity and autophagy, and NAC1-mediated ROCK1 appears to control both.

It is now widely acknowledged that T cell memory is crucial for the host's immune response to pathogens such as viruses. Several transcriptional factors have been identified as influencing T cell memory formation. However, until our recent finding on the NAC1-mediated regulation of CD8$^{+}$ T cell memory formation [16], there has been no investigation on how NAC1 regulates T cell memory formation. NAC1$^{-/-}$ CD4$^{+}$ T cells maintain lower metabolism (Figure 1E–1H), and this lower metabolism likely meets memory T cells' resting requirement and prolongs their survival. In this study, we observed a similar phenomenon that the absence of NAC1 in mice resulted in a higher frequency of VACV-specific CD4$^{+}$ T cell memory formation (Figure 5). Furthermore, the adoptive transferred NAC1$^{-/-}$ CD4$^{+}$ T cells displayed better survival rates than WT CD4$^{+}$ T cells (Figure 6 & Figure S4), indicating that NAC1 suppresses the formation of antigen-specific CD4$^{+}$ memory T cells. Additionally, we noted that the frequency of VACV-specific donor T cells was significantly increased when recipient mice were treated with the irradiation (Figure 6B & Figure S4A), most likely due to the prolonged clearance period of the VACV in the irradiation-treated mice, as many endogenous T cells might have been eliminated during irradiation. From the results shown in Figure 6B, Figure 7D and Figure S4A, we found that these VACV-specific memory T cells are more likely to survive in the tissue-resident memory status (CD44$^{high}$CD69$^{high}$CD197$^{low}$). Interestingly, overexpression of ROCK1 in NAC1$^{-/-}$ CD4$^{+}$ T cells reversed the increased CD4$^{+}$ memory T cell formation (Figure 7D-7F).

How mTOR and autophagy impact T cell memory is currently under extensive investigation. For instance, mTOR inhibitors like rapamycin have been found to enhance the formation of viral-specific T cell memory [35,36], which is consistent with our findings that NAC1$^{-/-}$ CD4$^{+}$ T cells defective mTOR signaling display increased viral-specific T cell memory formation. However, the impact of autophagy on T cell memory formation is still controversial. Some studies showed that autophagy benefits liver resident CD8$^{+}$ T cell maintenance [37], while

Author Manuscript Author Manuscript Author Manuscript Author Manuscript

others found that autophagy deficiency leads to upregulation of effector $CD8^+$ memory T cells [38]. We observed in this study that autophagy-deficient $NAC1^{-/-}$ $CD4^+$ T cells exhibit increased VACV-specific memory T cell formation, suggesting a role of NAC1 in suppressing $CD4^+$ T cell memory through both mTOR and autophagy regulation. One limitation of this study is that we only used the vaccinia virus as the tool to challenge the host and examine the antigen-specific T-cell memory performance. Other types of respiratory viruses might show a similar pattern if applied. The findings of this study may lay a foundation for the study of whether targeting NAC1 could boost T cell memory formation and prolong the efficacy of several vaccinations (e.g., COVID vaccine) that maintain relatively short protection periods. Furthermore, since $NAC1^{-/-}$ T cells have different glycolysis and oxidative profiles, targeting NAC1 to boost memory T cell-based immunotherapy may improve its efficiency in treating cancers.

## Supplementary Material

Refer to Web version on PubMed Central for supplementary material.

## Acknowledgments:

We thank Dr. Jianlong Wang at Columbia University Irving Medical Center for providing $NAC1^{-/-}$ mice. We acknowledge Ms. Robbie Moore from The School of Medicine Cell Analysis Facility (SOM-CAF) at the Texas A&M Health Science Center. We thank Dr. Malea Murphy from Integrated Microscope and Imaging Laboratory at Texas A&M Health Science Center. We acknowledge Dr. Stanislav Vitha and Rick Littleton from Microscope and Imaging Center at Texas A&M University.

### Funding:

This work was supported by National Institutes of Health Grant R01AI121180, R21AI167793, R01CA221867, and R01CA273002 to J. S. and J-M.Y., and Department of Defense Grant LC210150 to J.S.

## Data Availability Statement:

The data presented in this study are available on request from the corresponding author.

## Reference

1. Medzhitov R Recognition of microorganisms and activation of the immune response. Nature 2007;449(7164):819–826. [PubMed: 17943118]
2. Lauvau G, Soudja SM. Mechanisms of Memory T Cell Activation and Effective Immunity. Adv Exp Med Biol 2015;850:73–80. [PubMed: 26324347]
3. Tartof SY, Slezak JM, Fischer H, et al. Effectiveness of mRNA BNT162b2 COVID-19 vaccine up to 6 months in a large integrated health system in the USA: a retrospective cohort study. Lancet 2021;398(10309):1407–1416. [PubMed: 34619098]
4. Eichner M Analysis of historical data suggests long-lasting protective effects of smallpox vaccination. Am J Epidemiol 2003;158(8):717–723. [PubMed: 14561660]
5. Baxter R, Ray P, Tran TN, et al. Long-term effectiveness of varicella vaccine: a 14-Year, prospective cohort study. Pediatrics 2013;131(5):e1389–1396. [PubMed: 23545380]
6. Haque M, Song J, Fino K, et al. C-Myc regulation by costimulatory signals modulates the generation of CD8+ memory T cells during viral infection. Open Biol 2016;6(1):150208. [PubMed: 26791245]

Author Manuscript Author Manuscript Author Manuscript Author Manuscript


7. Avery L, Filderman J, Szymczak-Workman AL, Kane LP. Tim-3 co-stimulation promotes short-lived effector T cells, restricts memory precursors, and is dispensable for T cell exhaustion. Proc Natl Acad Sci U S A 2018;115(10):2455–2460. [PubMed: 29463725]
8. Chen Y, Zander R, Khatun A, Schauder DM, Cui W. Transcriptional and Epigenetic Regulation of Effector and Memory CD8 T Cell Differentiation. Front Immunol 2018;9:2826. [PubMed: 30581433]
9. Harberts A, Schmidt C, Schmid J, et al. Interferon regulatory factor 4 controls effector functions of CD8(+) memory T cells. Proc Natl Acad Sci U S A 2021;118(16).
10. Korutla L, Wang P, Jackson TG, Mackler SA. NAC1, a POZ/BTB protein that functions as a corepressor. Neurochem Int 2009;54(3–4):245–252. [PubMed: 19121354]
11. Xia Z, Xu G, Nie L, et al. NAC1 Potentiates Cellular Antiviral Signaling by Bridging MAVS and TBK1. J Immunol 2019;203(4):1001–1011. [PubMed: 31235549]
12. Kim J, Chu J, Shen X, Wang J, Orkin SH. An extended transcriptional network for pluripotency of embryonic stem cells. Cell 2008;132(6):1049–1061. [PubMed: 18358816]
13. Faiola F, Yin N, Fidalgo M, et al. NAC1 Regulates Somatic Cell Reprogramming by Controlling Zeb1 and E-cadherin Expression. Stem Cell Reports 2017;9(3):913–926. [PubMed: 28781078]
14. Malleshaiah M, Padi M, Rue P, Quackenbush J, Martinez-Arias A, Gunawardena J. Nac1 Coordinates a Sub-network of Pluripotency Factors to Regulate Embryonic Stem Cell Differentiation. Cell Rep 2016;14(5):1181–1194. [PubMed: 26832399]
15. Yang JM, Ren Y, Kumar A, et al. NAC1 modulates autoimmunity by suppressing regulatory T cell-mediated tolerance. Sci Adv 2022;8(26):eabo0183. [PubMed: 35767626]
16. Wang L, Kumar A, Das JK, et al. Expression of NAC1 Restrains the Memory Formation of CD8(+) T Cells during Viral Infection. Viruses 2022;14(8).
17. Ylä-Anttila P, Vihinen H, Jokitalo E, Eskelinen EL. Monitoring autophagy by electron microscopy in Mammalian cells. Methods Enzymol 2009;452:143–164. [PubMed: 19200881]
18. Gawriluk TR, Ko C, Hong X, Christenson LK, Rucker EB 3rd. Beclin-1 deficiency in the murine ovary results in the reduction of progesterone production to promote preterm labor. Proc Natl Acad Sci U S A 2014;111(40):E4194–4203. [PubMed: 25246579]
19. Hofstee P, McKeating DR, Bartho LA, Anderson ST, Perkins AV, Cuffe JSM. Maternal Selenium Deficiency in Mice Alters Offspring Glucose Metabolism and Thyroid Status in a Sexually Dimorphic Manner. Nutrients 2020;12(1).
20. Narayanan KL, Chopra V, Rosas HD, Malarick K, Hersch S. Rho Kinase Pathway Alterations in the Brain and Leukocytes in Huntington's Disease. Mol Neurobiol 2016;53(4):2132–2140. [PubMed: 25941073]
21. Cotter CA, Earl PL, Wyatt LS, Moss B. Preparation of Cell Cultures and Vaccinia Virus Stocks. Curr Protoc Mol Biol 2017;117:16.16.11–16.16.18.
22. Kurachi M, Kurachi J, Chen Z, et al. Optimized retroviral transduction of mouse T cells for in vivo assessment of gene function. Nat Protoc 2017;12(9):1980–1998. [PubMed: 28858287]
23. Chi H. Regulation and function of mTOR signalling in T cell fate decisions. Nat Rev Immunol 2012;12(5):325–338. [PubMed: 22517423]
24. Wei J, Long L, Yang K, et al. Autophagy enforces functional integrity of regulatory T cells by coupling environmental cues and metabolic homeostasis. Nat Immunol 2016;17(3):277–285. [PubMed: 26808230]
25. Zhang Y, Yang JW, Ren X, Yang JM. NAC1 and HMGB1 enter a partnership for manipulating autophagy. Autophagy 2011;7(12):1557–1558. [PubMed: 22024751]
26. Gurkar AU, Chu K, Raj L, et al. Identification of ROCK1 kinase as a critical regulator of Beclin1-mediated autophagy during metabolic stress. Nat Commun 2013;4:2189. [PubMed: 23877263]
27. Zhang M, Jin X, Sun R, et al. Optimization of metabolism to improve efficacy during CAR-T cell manufacturing. J Transl Med 2021;19(1):499. [PubMed: 34876185]
28. Wang L, Das JK, Kumar A, et al. Autophagy in T-cell differentiation, survival and memory. Immunol Cell Biol 2021;99(4):351–360. [PubMed: 33141986]
29. Hildeman DA, Zhu Y, Mitchell TC, et al. Activated T cell death in vivo mediated by proapoptotic bcl-2 family member bim. Immunity 2002;16(6):759–767. [PubMed: 12121658]

Author Manuscript Author Manuscript Author Manuscript Author Manuscript

30. Hedrick SM, Ch'en IL, Alves BN. Intertwined pathways of programmed cell death in immunity. Immunol Rev 2010;236:41–53. [PubMed: 20636807]
31. Huang H, Lee SH, Sousa-Lima I, et al. Rho-kinase/AMPK axis regulates hepatic lipogenesis during overnutrition. J Clin Invest 2018;128(12):5335–5350. [PubMed: 30226474]
32. Shi J, Surma M, Wei L. Disruption of ROCK1 gene restores autophagic flux and mitigates doxorubicin-induced cardiotoxicity. Oncotarget 2018;9(16):12995–13008. [PubMed: 29560126]
33. Whang MI, Tavares RM, Benjamin DI, et al. The Ubiquitin Binding Protein TAX1BP1 Mediates Autophagasome Induction and the Metabolic Transition of Activated T Cells. Immunity 2017;46(3):405–420. [PubMed: 28314591]
34. Ganley IG, Lam du H, Wang J, Ding X, Chen S, Jiang X. ULK1.ATG13.FIP200 complex mediates mTOR signaling and is essential for autophagy. J Biol Chem 2009;284(18):12297–12305. [PubMed: 19258318]
35. Araki K, Turner AP, Shaffer VO, et al. mTOR regulates memory CD8 T-cell differentiation. Nature 2009;460(7251):108–112. [PubMed: 19543266]
36. Ye L, Lee J, Xu L, et al. mTOR Promotes Antiviral Humoral Immunity by Differentially Regulating CD4 Helper T Cell and B Cell Responses. J Virol 2017;91(4).
37. Swadling L, Pallett LJ, Diniz MO, et al. Human Liver Memory CD8(+) T Cells Use Autophagy for Tissue Residence. Cell Rep 2020;30(3):687–698.e686. [PubMed: 31968246]
38. DeVorkin L, Pavey N, Carleton G, et al. Autophagy Regulation of Metabolism Is Required for CD8(+) T Cell Anti-tumor Immunity. Cell Rep 2019;27(2):502–513.e505. [PubMed: 30970253]

Author Manuscript Author Manuscript Author Manuscript Author Manuscript

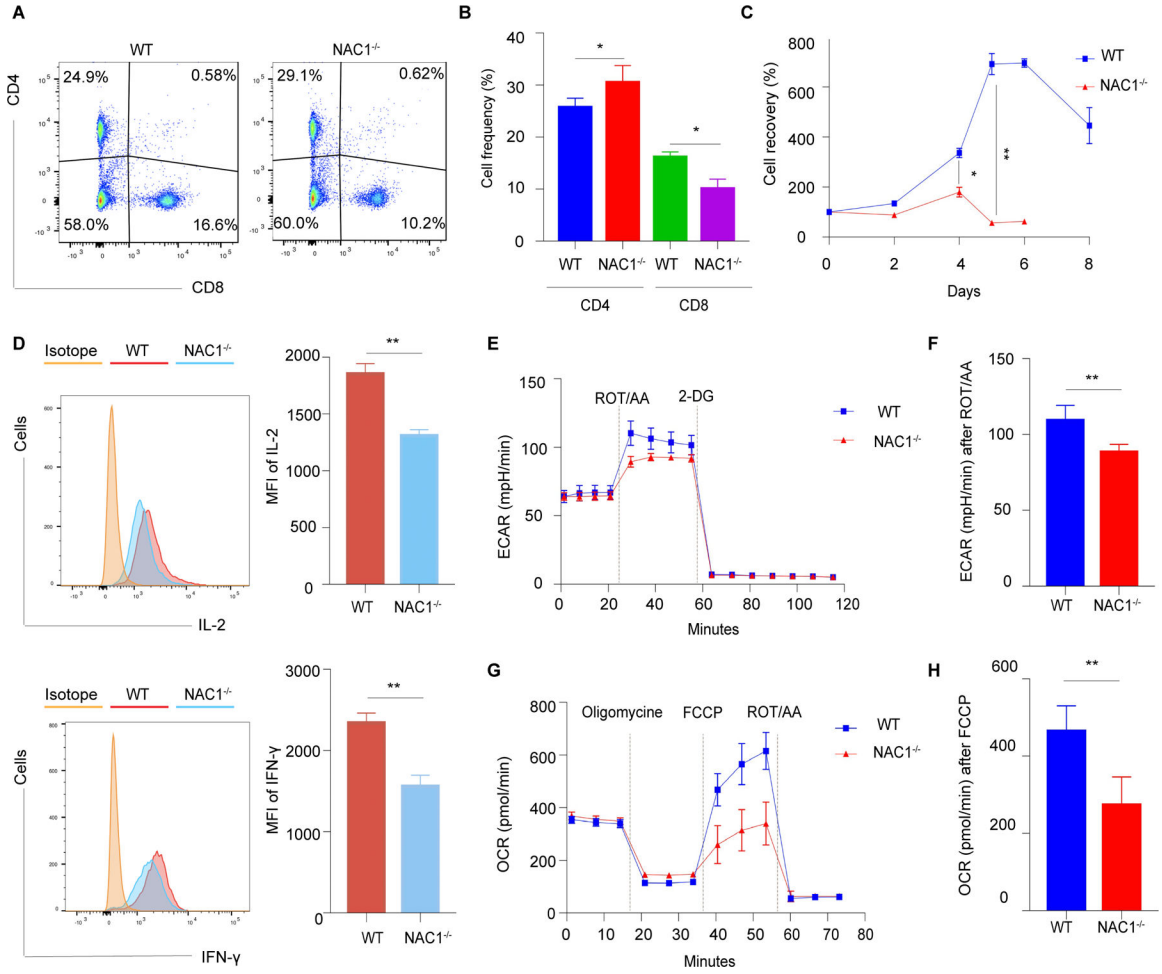


**Figure 1. Loss of NAC1 alters the survival, function, and metabolism of CD4$^+$ T cells.**

(**A&B**) T cells from pooled LNs and spleen of WT and NAC1$^{-/-}$ mice were analyzed by flow cytometry for cell frequency. The data shown are representative of five mice per group of three independent experiments. *, $p < 0.05$. (**C-H**) Purified CD4$^+$ T cells were isolated from WT and NAC1$^{-/-}$ mice and stimulated with coated anti-CD3 Ab and soluble anti-CD28 Ab. The plotting data shown are representative of three identical experiments. (**C**) The cell recovery was examined with trypan blue exclusion from day 0 to day 8. The frequency of T cells on day 0 was assigned a value of 100%. *, $p < 0.05$; **, $p < 0.01$. Repeats n= 4. (**D**) T cells were stimulated, and intracellular cytokines (IL-2 and IFN-γ) were analyzed through flow cytometry. Repeats n=3. (**E&F**) 2X10$^5$ stimulated CD4$^+$ T cells were seeded into Seahorse XF96 culture plate. The Extracellular Acidification Rate (ECAR) was monitored with Rotenone and Antimycin A (ROT/AA), 2-deoxy-glucose (2-DG) drugs injection at different time points in the figure. Sample number (n=4), **, $p < 0.01$. (**G&H**) 2X10$^5$ stimulated CD4$^+$ T cells were seeded into Seahorse XF96 culture plate. The Oxygen Consumption Rate (OCR) was measured with Oligomycin, Carbonyl cyanide-4 (trifluoromethoxy) phenylhydrazone (FCCP), Rotenone and Antimycin A (ROT/AA) drugs injections at different time points in the figure. Sample number (n=4), **, $p < 0.01$.

Author Manuscript Author Manuscript Author Manuscript Author Manuscript

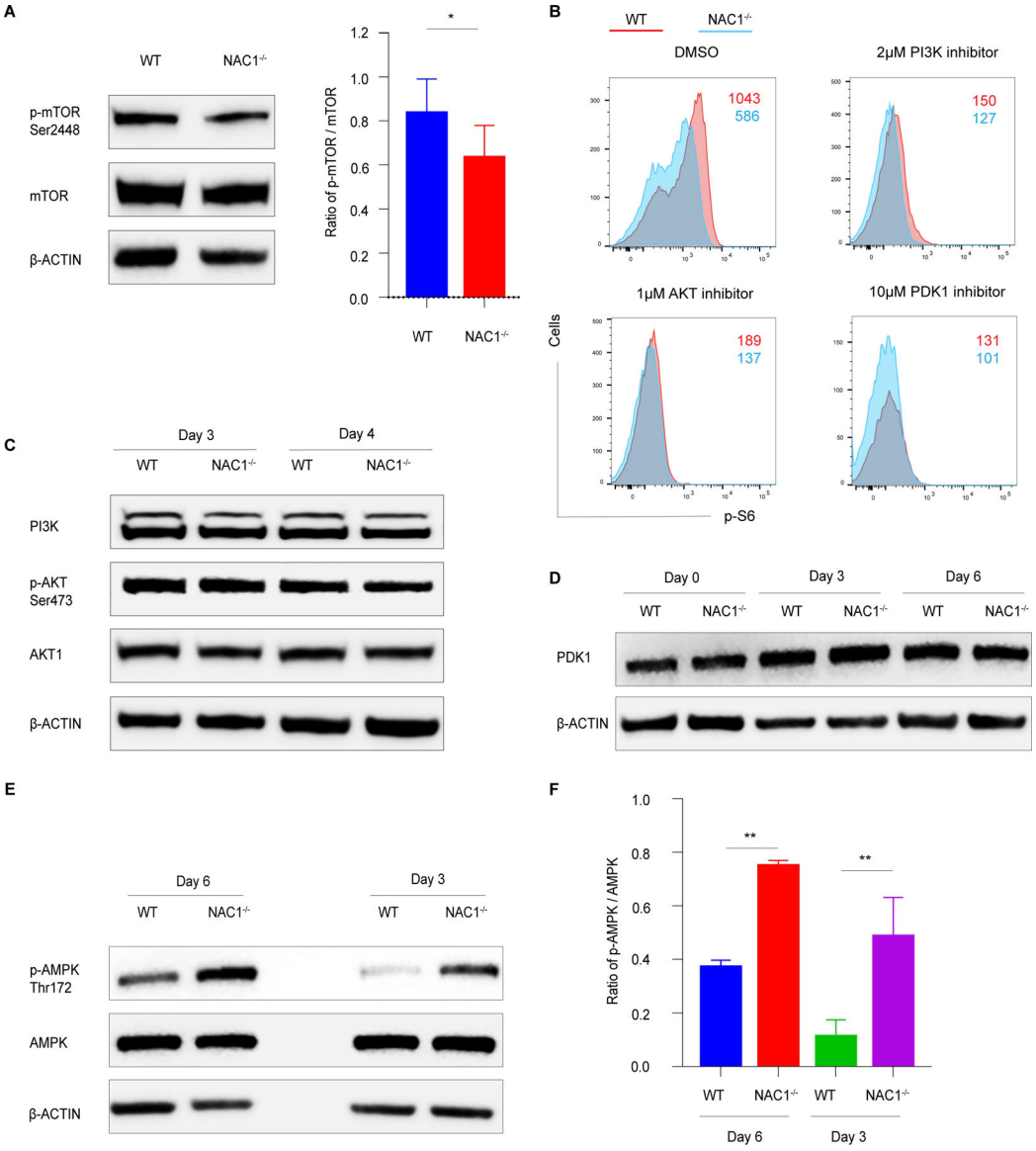


**Figure 2. NAC1 regulates glycolysis of CD4$^+$ T cells through the AMPK-mTOR pathway.**

CD4$^+$ T cells were isolated from the pooled LNs and spleen of WT and NAC1$^{-/-}$ mice and activated with coated anti-CD3 Ab and soluble anti-CD28 Ab. Proteins were extracted from the cells on different days. (**A**) p-mTOR/ mTOR activity was checked by immunoblots on day 3. The blot images are representative of three identical experiments. *, $p < 0.05$. (**B**) The activated T cells were treated with DMSO, dactolisib (PI3K inhibitor), MK-2206 2HCl (AKT inhibitor), OSU-03012 (PDK1 inhibitor) according to the concentration indicated in the figures. p-S6 protein was analyzed by flow cytometry using intracellular staining on day 0. Mean Fluorescence intensity (MFI) was calculated. Repeats n=3. (**C**) PI3K and AKT expression were tested by immunoblots. Repeats n=3. (**D**) PDK1 expressions were verified on day 0, day 3, and day 6. Repeats n=3. (**E-F**) AMPK activity was checked on day 3 and day 6. The ratio of AMPK/ p-AMPK is calculated by ImageJ. The blot images are representative of three identical experiments. **, $p < 0.01$.

Author Manuscript Author Manuscript Author Manuscript Author Manuscript

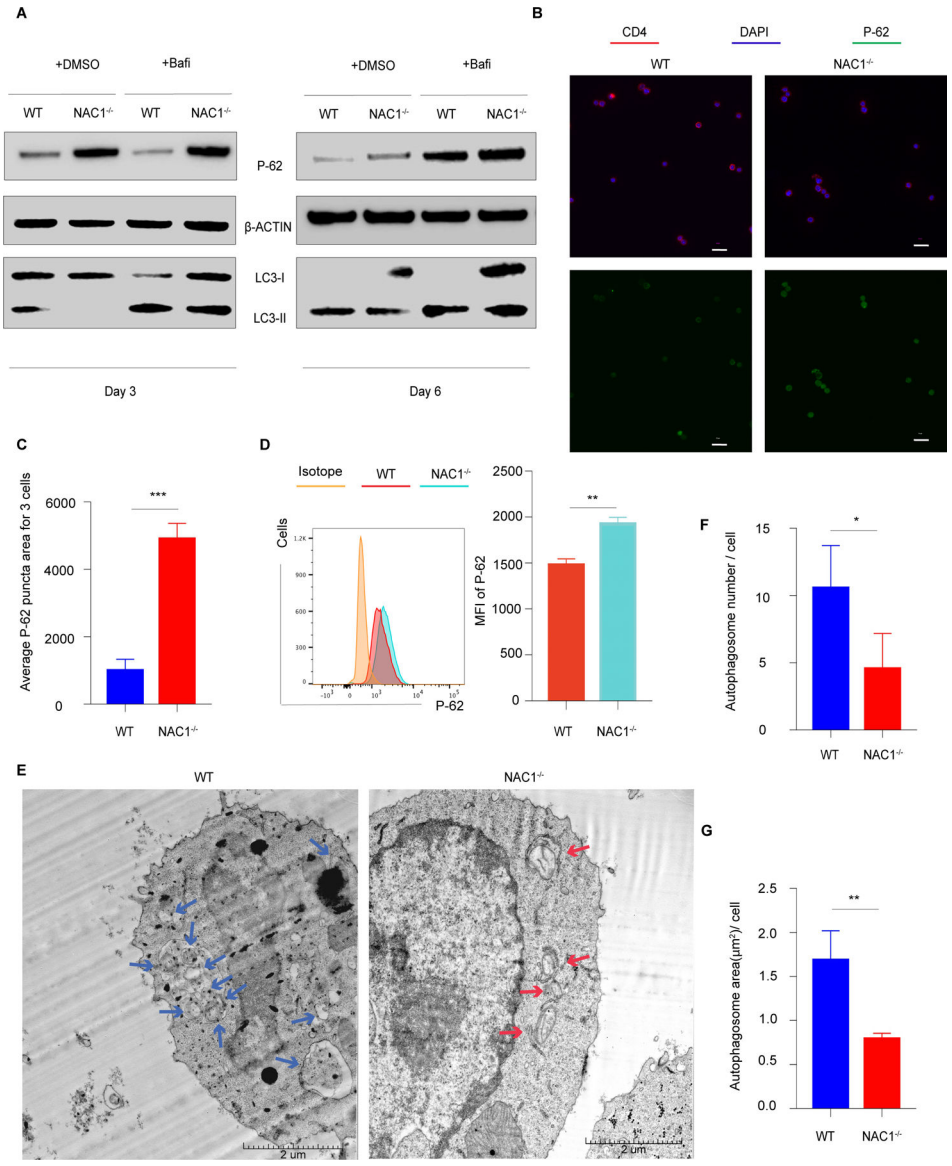


**Figure 3. Effect of NAC1 expression on autophagy in CD4$^+$ T cells.**

CD4$^+$ T cells were isolated from the pooled LNs and spleen of WT or NAC1$^{-/-}$ mice and stimulated with coated anti-CD3 Ab and soluble anti-CD28 Ab. (**A**) Cells were cultured with either DMSO (Control) or bafilomycin for 2 hours before protein extraction on day 3 and day 6. Autophagic adaptor proteins, including both P-62 and LC3, were analyzed by immunoblot. The blot images are representative of three identical experiments. (**B-D**) Purified CD4$^+$ T cells were cultured for 3 days. Repeats n=3. (**B&C**) Confocal microscope analysis on P-62 expression. Cells were stained with CD4 marker (Red), nucleus (Blue), and P-62 (Green). The scale bar is 20 μm. The green puncta for 3 cells were accumulated together for comparison. ***, $p < 0.001$. An unpaired student T-test was used for quantification. (**D**) P-62 MFI was analyzed by flow cytometry. (**E-G**) Autophagosome formation was checked by transmission electron microscope (TEM). The scale bar is 2 μm. Both autophagosome numbers and area were calculated and quantified based on more than

10 micrographics. Blue arrows or red arrows were used to indicate the autophagosome in WT or NAC1$^{-/-}$ CD4$^{+}$ T cells. *, $p < 0.05$; **, $p < 0.01$.

Author Manuscript Author Manuscript Author Manuscript Author Manuscript

Author Manuscript Author Manuscript Author Manuscript Author Manuscript

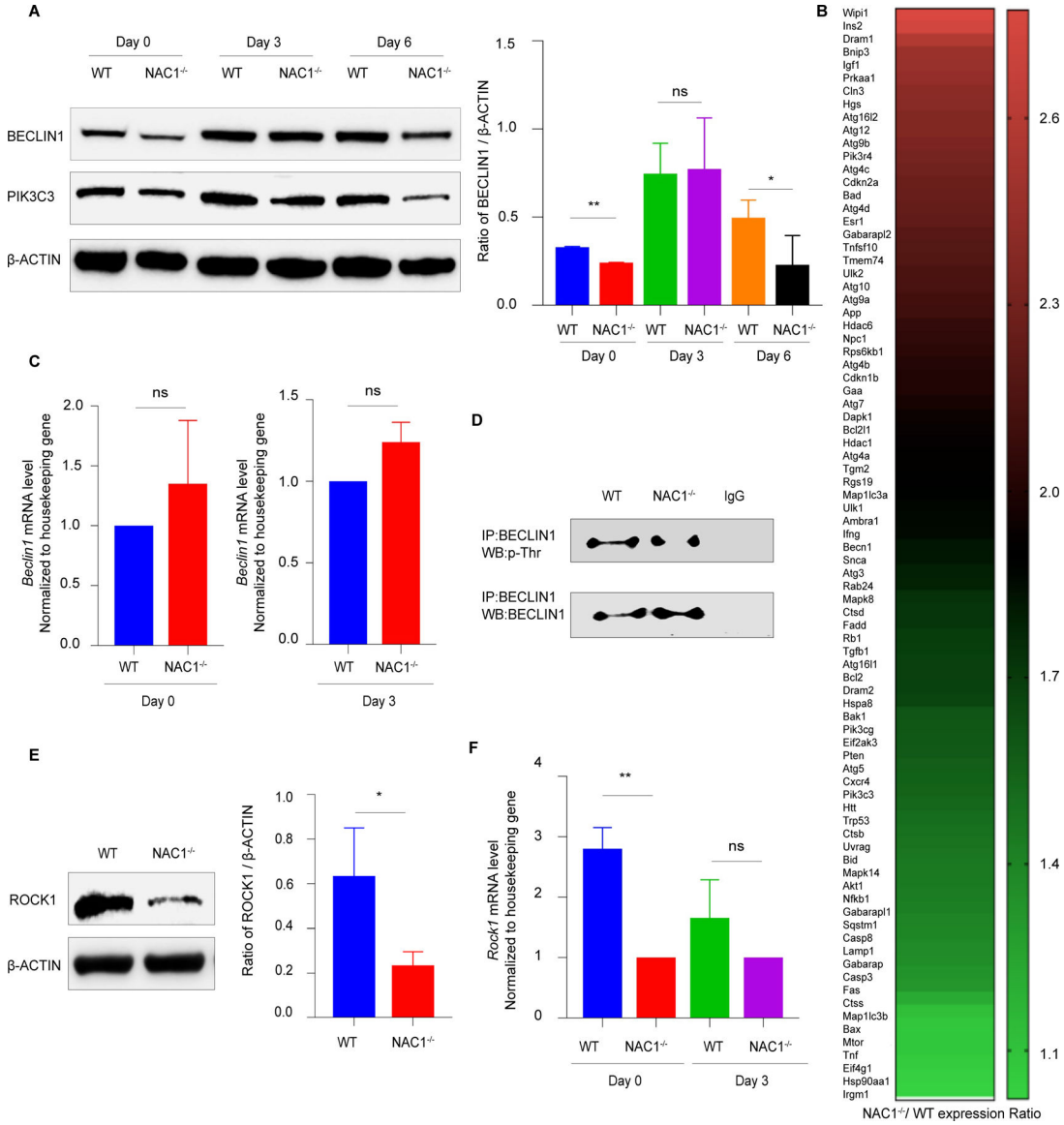


**Figure 4. NAC1 regulates autophagy of CD4$^+$ T cells through ROCK1-mediated phosphorylation of BECLIN1.**

(**A**) The BECLIN1 and PIK3C3 expression on day 0, day 3, and day 6. T cells were activated, and proteins were extracted from the activated cells on different days. The ratio of BECLIN1/ β-ACTIN was calculated by ImageJ. The blot images are representative of three identical experiments. *, $p < 0.05$; **, $p < 0.01$; ns, $p > 0.05$. (**B**) T cells mRNA was extracted from activated T cells on day 0. cDNA was used for Autophagy Pathway RNA Microarray. mRNA expression ratio of NAC1$^{-/-}$ / WT had displayed among 84 autophagy pathway-related genes. Repeats n=3. (**C**) *Beclin1* mRNA expression was confirmed on day 0 and day 3 by qPCR. ns, $p > 0.05$. Sample number = 4. (**D**) T cell proteins were extracted from either WT or NAC1$^{-/-}$ CD4$^+$ T cells on day 3 for immunoprecipitation with either anti-BECLIN1 or anti-IgG antibodies. The eluted fractions were detected with anti-p-Threonine and anti-BECLIN1 immunoblots. Repeats n=3. (**E**) The ROCK1 protein expression was detected by immunoblot. Repeats n=3. *, $p < 0.05$ (**F**) The *Rock1* mRNA

Author Manuscript Author Manuscript Author Manuscript Author Manuscript

expression was quantified by qPCR on day 0 and day 3. Sample number = 4. **, $p < 0.01$; ns, $p > 0.05$.

Author Manuscript Author Manuscript Author Manuscript Author Manuscript

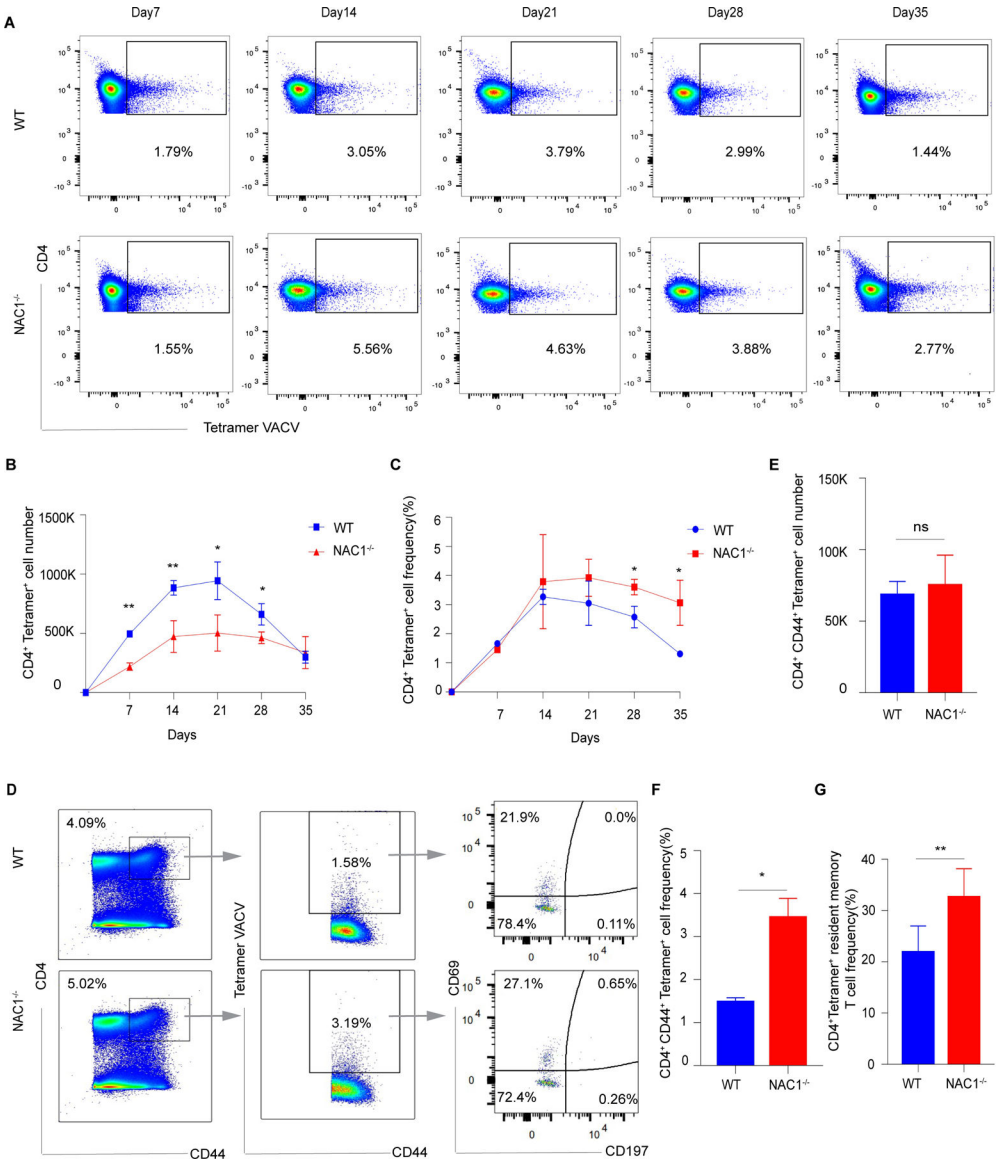


**Figure 5. NAC1$^{-/-}$ mice sustain higher survival of VACV-specific CD4$^{+}$ T cells and enhance formation of the VACV-specific memory CD4$^{+}$ T cells.**

WT or NAC1$^{-/-}$ mice were infected with the vaccinia virus (VACV) at 2X10$^{6}$ PFU. The VACV-infected mice were sacrificed at 1,2,3,4,5 weeks to get the pooled LNs and spleen. Then the tissue was smashed and filtered with 40 μm cell strainers. The red blood cells were removed by RBC lysis buffer. The total cell number for each mouse was calculated by cell counter. Multiple cell surface markers (CD4, CD44, CD69, CD197) and VACV tetramer staining were applied before flow cytometry analysis. The representative data are three identical experiments. Mice number for each group (n=5–7). (**A**) Representative flow cytometry plotting for those VACV-specific CD4$^{+}$ T cells during 1 to 5 weeks. (**B**) VACV-specific CD4$^{+}$ T cell number change in 35 days. (**C**) VACV-specific CD4$^{+}$ T cell frequency survival in 35 days. (**D**) Representative flow cytometry for VACV-specific memory CD4$^{+}$ T cells and memory subsets analysis on day 35. (**E**) VACV-specific memory CD4$^{+}$ T cell number on day 35. (**F**) VACV-specific memory CD4$^{+}$ T cell frequency on day 35. (**G**)

Author Manuscript Author Manuscript Author Manuscript Author Manuscript

VACV-specific resident-memory $CD4^+$ T cell ($CD44^{high}CD69^{high}CD197^{low}$) frequency on day 35. *, $p < 0.05$; **, $p < 0.01$; ns, $p > 0.05$.

Author Manuscript Author Manuscript Author Manuscript Author Manuscript

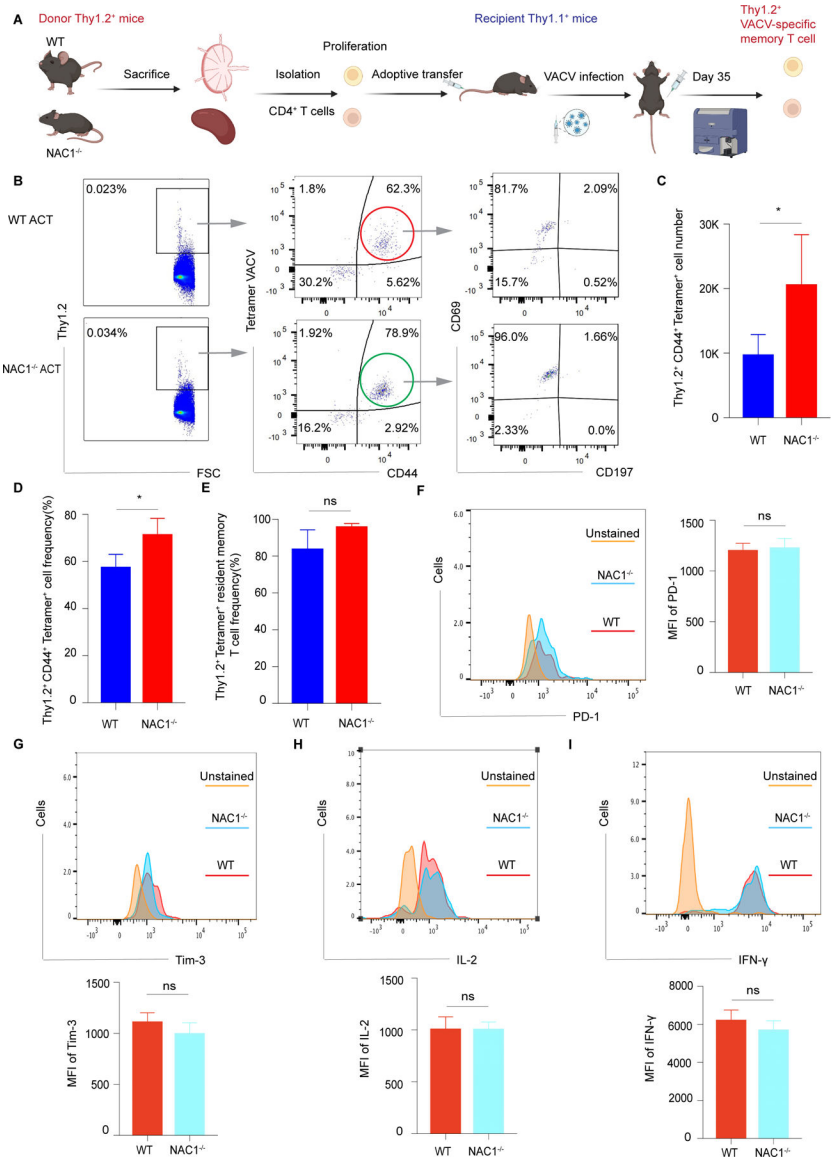


**Figure 6. Adoptive transferred NAC1$^{-/-}$ CD4$^{+}$ T cells generate a higher number of memory T cells.**

Either WT or NAC1$^{-/-}$ mice (Thy1.2$^{+}$) were sacrificed as the donor mice. Then the naive CD4$^{+}$ T cells were purified from pooled LNs and spleen. The WT or NAC1$^{-/-}$ CD4$^{+}$ T cells were cultured for 3 days and 1X10$^{6}$ cells were adoptively transferred into randomly chosen recipient mice (Thy1.1$^{+}$) without irradiation treatment. The same day after ACT, mice were challenged with 2X10$^{6}$ PFU VACV. After 35 days, the pooled LNs and spleen were collected for flow cytometry analysis. Cells were stained with Thy1.2, CD44, CD69, and CD197 surface markers and VACV tetramer staining. The representative data are three identical experiments. Mice number for each group (n=5). (**A**) The diagram for the experiment design. (**B**) Representative flow cytometry for the donor VACV-specific memory T cells and memory subsets on day 35. (**C**) Donor VACV-specific memory T cell number. (**D**) Donor VACV-specific memory T cell frequency. (**E**) Donor VACV-specific resident-memory T cell frequency. *, $p < 0.05$; ns, $p > 0.05$. (**F&G**) VACV-specific memory T cell

exhaustion marker PD-1, Tim-3 expression. Repeats n=3. (**H&I**) VACV-specific memory T cell functional cytokines, IL-2 and IFN-γ secretion. Repeats n=3.

Author Manuscript Author Manuscript Author Manuscript Author Manuscript

Author Manuscript Author Manuscript Author Manuscript Author Manuscript

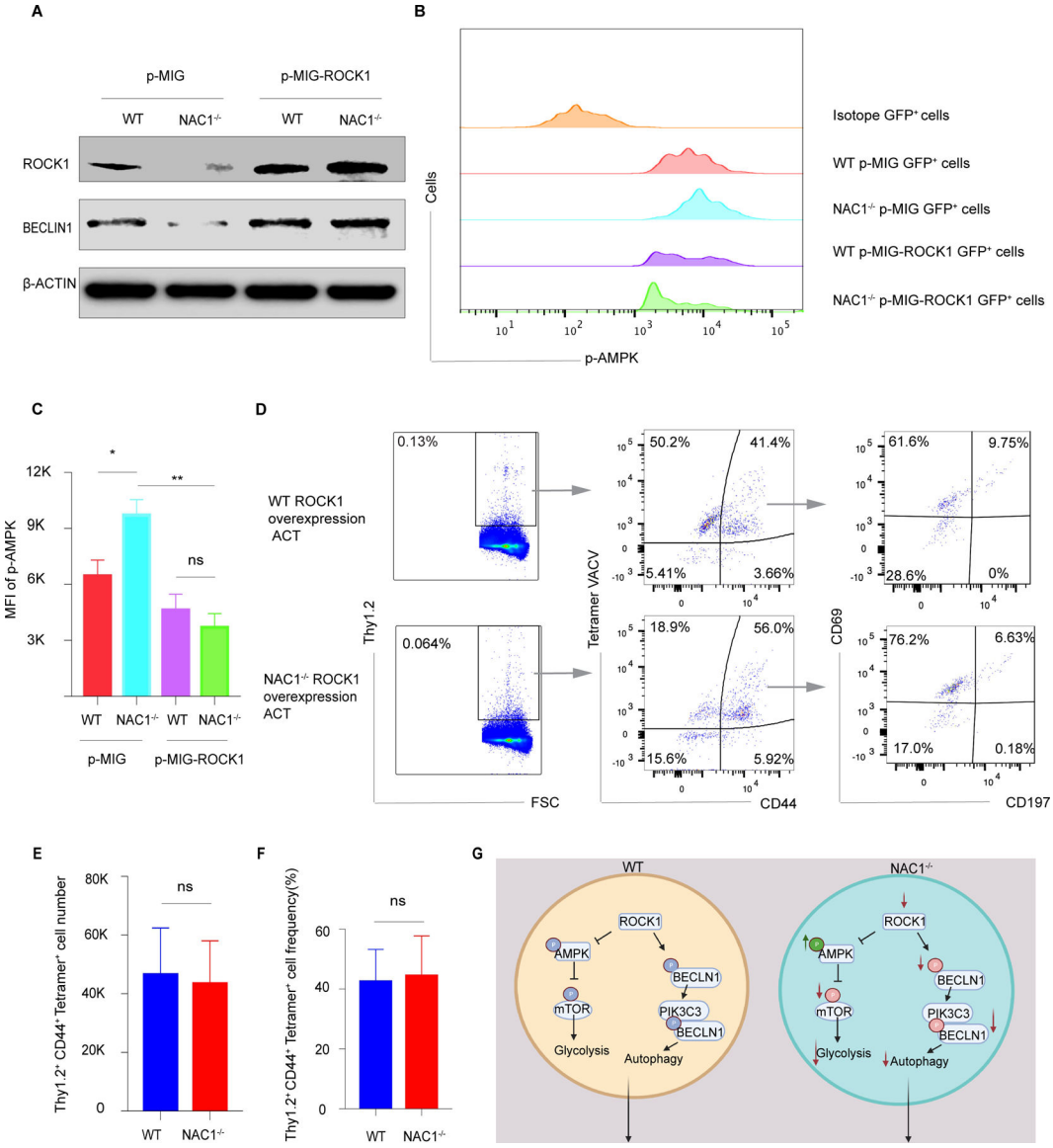


**Figure 7. Effect of overexpression of ROCK1 on memory T cell formation in NAC1$^{-/-}$ CD4$^{+}$ T cells.**

The naive WT or NAC1$^{-/-}$ CD4$^{+}$ T cells were purified from pooled LNs and spleen. T cells were transduced with either empty p-MIG or p-MIG-ROCK1 retrovirus vector. Then the GFP$^{+}$ cells were sorted out for experiments. (**A**) BECLIN1 expression was examined by immunoblot. Repeats n=3. (**B&C**) p-AMPK expression was verified by flow cytometry after intracellular staining. The MFI of p-AMPK was calculated and compared. The plotting data shown are representative of three identical experiments (n=3). *, $p < 0.05$; **, $p < 0.01$; ns, $p > 0.05$. (**D-F**) 2X10$^{5}$ ROCK1 overexpressed WT or NAC1$^{-/-}$ CD4$^{+}$ T cells (donor Thy1.2$^{+}$) were adoptively transferred into randomly chosen irradiated treatment recipient mice (Thy1.1$^{+}$). Then the mice were challenged with 2X10$^{6}$ PFU VACV. The representative data are three identical experiments. Mouse number for each group (n=5). (**D**) Representative flow cytometry plotting for the donor VACV-specific memory T cells and memory subsets on day 35. (**E**) Donor VACV-specific memory T cell number. (**F**) Donor

VACV-specific memory T cell frequency. (**G**) Proposed model of $CD4^+$ T cell memory formation regulated by NAC1.

Author Manuscript Author Manuscript Author Manuscript Author Manuscript